


## A hybrid numerical model for long-range electromagnetic wave propagation

Gül Yesa ALTUN<sup>1,2</sup>, Özlem ÖZGÜN<sup>2,\*</sup> 

<sup>1</sup>Department of Communication and Information Technologies, Aselsan Inc., Ankara, Turkey

<sup>2</sup>Department of Electrical and Electronics Engineering, Hacettepe University, Ankara, Turkey

Received: 03.06.2021

Accepted/Published Online: 28.07.2021

Final Version: 30.11.2021

**Abstract:** A hybrid numerical model is presented for solving long range electromagnetic wave propagation problems involving objects on or above the ground surface by hybridizing the two-way split-step parabolic equation (2W-SSPE) method with the method of moments (MoM). The advantages of the proposed model are twofold: (i) It reduces the staircasing error in irregular terrain modeling, which usually occurs when the standard SSPE method is used alone. This is achieved by employing the MoM to more accurately obtain the scattered fields from slanted/curved surfaces. (ii) It enables the SSPE method to handle the problems involving objects above the Earth's surface, which cannot be easily modeled by the standard SSPE method due to difficulty in imposing boundary conditions. The accuracy of the hybrid method is numerically verified by comparing the numerical results with those of the 2W-SSPE and the GO+UTD (geometric optic + uniform theory of diffraction) methods in some representative propagation problems.

**Key words:** Parabolic equation, electromagnetic wave propagation, hybrid method, method of moments, split-step parabolic equation method, terrain effects

### 1. Introduction

Tropospheric electromagnetic wave propagation is an important part of wireless communication and radar technologies. The behavior of electromagnetic waves in propagation problems is affected by many factors, such as frequency, inhomogeneous atmosphere, Earth's surface, terrain irregularities, etc. The analytical or numerical solution of such problems is often difficult, especially in real-life propagation scenarios, because of the complex interaction of several wave components (i.e. reflection, refraction and diffraction) that must be included in the solution. Since the distances involved in long-range propagation problems are very large compared to the wavelength, the numerical solution of these problems with conventional full-wave methods (such as finite element method – FEM or method of moments – MoM) is a challenging task because of the large electrical size of the computational domain. Therefore, developing efficient computational approaches has gained great importance owing to the advancements in computer technology.

The parabolic equation (PE) method [1], which is based on the paraxial approximation of the Helmholtz equation, is one of the most reliable numerical method for modeling long-range propagation problems. The PE is numerically solved by formulating the problem as an initial value problem. That is, the initial field is defined at a specific range (usually at the location of the antenna), which is then moved through the range by applying stepwise Fourier transformations to the fields. Due to the nature of the implementation scheme, this method is known as Fourier-based split-step parabolic equation (SSPE) method [2]. The standard SSPE method is a

\*Correspondence: ozlem@ee.hacettepe.edu.tr

one-way method; this means that the fields move only in the forward direction. The standard SSPE method has been widely used to model the light propagation in optical fibers [3], the acoustic wave propagation under the sea [4], and the electromagnetic wave propagation in the troposphere [5–11]. One of the major reasons why this method is preferred is that larger range steps can be used (as opposed to full-wave solvers that typically use one tenth of a wavelength as step size), and hence, long-range propagation problems can easily be solved with reduced computational load. Another advantage of the SSPE method is its ability in handling inhomogeneous atmospheric conditions in the troposphere. In the early periods of this method, the narrow-angle approximation was used in the PE formulation, by assuming that small propagation angles (up to  $10^\circ - 15^\circ$  from the paraxial direction) are often encountered in long range problems. However, larger propagation angles need to be included in the solution to handle irregular terrain including valleys and hills with steep slopes. For this purpose, wide angle propagators were used in order to extend the propagation angles up to  $40^\circ - 45^\circ$  [12, 13].

Another breakthrough was made by developing the two-way SSPE (2W-SSPE) to model both forward and backward propagating fields in order to incorporate multipath effects into the solution. In [14], the 2W-SSPE is implemented in a way that when the field meets the staircase-approximated terrain, it is reflected from the terrain surface and propagated in both forward and backward directions. At each time the field hits the terrain, it is split into forward and backward propagating fields, each of which travels along its own direction. This recursive process continues until the field exits the computational domain or a certain threshold is reached. The 2W-SSPE method was implemented in an open-source software, called PETOOL [15, 16], which was then used in various studies [17–20]. Although terrain modeling with a staircase approximation provides reliable results in most situations, the accuracy of the 2W-SSPE method might degrade if there are curved/slanted surfaces over the terrain profile. Another issue in the standard SSPE modeling is that boundary conditions cannot be imposed automatically over Earth's surface. For example, to satisfy the boundary conditions over a perfectly conducting ground, odd and even symmetric profiles of the vertical field are constructed for Dirichlet (soft) and Neumann (hard) boundary conditions, respectively, by employing the image theory. Hence, the SSPE methods cannot easily handle problems that include objects above the ground (i.e. objects which do not touch the ground), because of the difficulty to include the effect of multiple images used to model the interaction between nontouching objects and the ground. For this reason, the SSPE modeling was not used so far in propagation problems that involve objects above terrain, to the best knowledge of the authors.

In this paper, we present a hybrid method by combining the 2W-SSPE method with MoM to overcome the abovementioned challenges in a standard SSPE modeling. The staircasing error is eliminated, and hence, curved/slanted surfaces are modeled more accurately. In addition, the SSPE method is made applicable to problems involving objects above Earth's surface. The hybridization of the two methods is done as follows: The MoM is used to obtain the scattered fields from slanted/curved surfaces on or above Earth's surface, whereas the 2W-SSPE is used to propagate the fields over long distances. In this manner, a more accurate propagation model is developed by combining the advantages of both methods. Earlier in [21], we presented the very initial results of a different hybridization scheme by defining a subregion around the terrain/objects and by propagating the fields calculated by the MoM at the boundaries of this subregion. However, in this study, we propose an alternative hybridization scheme that has some advantages over [21] in terms of easier and more accurate modeling of atmospheric inhomogeneities in the subregion where MoM is used. These issues are discussed in the following sections.

This paper is organized as follows: Section 2 summarizes the basic principles of the SSPE methods, the

MoM and the proposed hybrid method. Section 3 presents some numerical examples. The performance of the proposed method is compared with the results of the 2W-SSPE and the geometric optic (GO) + uniform theory of diffraction (UTD) method [22]. Finally, Section 4 draws some conclusions. The suppressed time-dependence of the form  $\exp(-i\omega t)$  is assumed throughout the paper.

## 2. Formulation

### 2.1. SSPE methods

A two-dimensional electromagnetic propagation problem is illustrated in Figure 1a. The parabolic equation (PE) is approximated from the scalar Helmholtz equation by separating the rapidly-changing phase term from the solution and defining a reduced function which is slowly-changing over range. This approximation considers the propagation angles close to the horizontal (paraxial) direction. The reduced function is defined as  $u(x, z) = \exp(-ikx)\varphi(x, z)$ , where  $\varphi(x, z)$  represents the transverse component of the electric or magnetic field in horizontal (soft) or vertical (hard) polarization, respectively. The parabolic equation is obtained as [9]

$$\left[ \frac{\partial^2}{\partial x^2} + 2ik \frac{\partial}{\partial x} + \frac{\partial^2}{\partial z^2} + k^2(n^2 - 1) \right] u(x, z) = 0, \quad (1)$$

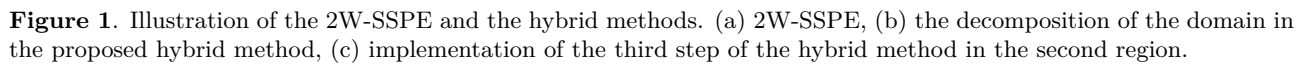
where  $k = 2\pi/\lambda$  is the wavenumber ( $\lambda$  is the wavelength),  $x$  and  $z$  are the range and height, respectively, and  $n$  is the refractive index.

In the standard PE approach, although the differential operator in (1) is factored into two pseudo-differential operators, each of which belongs to forward and backward propagating fields, only the operator corresponding to forward fields is considered. The PE is numerically solved by the Fourier-based split-step method. With wide-angle approximation, the split-step solution is expressed as [12]

$$u(x + \Delta x, z) = \exp[ik(n - 1)\Delta x]F^{-1} \left\{ \exp \left[ -\frac{ip^2\Delta x}{k} \left( \sqrt{1 - \frac{p^2}{k^2}} + 1 \right)^{-1} \right] F\{u(x, z)\} \right\}, \quad (2)$$

where  $F$  and  $F^{-1}$  indicate the Fourier transform and its inverse, respectively,  $p = k \sin \psi$  is the transform variable ( $\psi$  is the propagation angle from the paraxial direction), and  $\Delta x$  is the range step size.

The standard SSPE method is implemented as an initial-value problem by starting the algorithm from a specific range (usually at the location of an antenna) and moving forward in a stepwise manner. At each range step, the vertical field profile along height is determined by using (2). Although the standard SSPE method is applied in the forward direction only, terrain factors can still be handled even at the expense of ignoring backscattering fields by using a staircase-approximated terrain. In the standard SSPE, when the field hits the terrain, the vertical field profile that is computed by (2) is set to zero on the terrain, and then, propagated in the forward direction. The staircase approach works well in the approximate sense because the boundary conditions on the sloping features of the terrain profile may not be modeled accurately. Another important issue in the standard PE modeling is that boundary conditions cannot be handled automatically. Even in a simple case where the ground surface is perfectly conducting, the computation domain is extended from  $[0, z_{max}]$  to  $[-z_{max}, z_{max}]$  (where  $z_{max}$  refers to the maximum height), and the odd and even symmetric field profiles are included for Dirichlet (soft) and Neumann (hard) boundary conditions, respectively. Alternative approach is to convert the Fourier transform to one-sided discrete sine or cosine transforms, for Dirichlet and Neumann boundary conditions, respectively, by avoiding the height extension. The introduction of the odd and even



symmetric field profiles is based on the image theory. Although this approach can be used for irregular terrain profile, it cannot be applied to problems involving objects above the ground (i.e. objects which do not touch the ground) in a straightforward manner because of the need to incorporate the effect of multiple images when modeling the interaction between nontouching objects and the ground. Hence, there is not any study in the literature which applies the SSPE for problems involving objects above terrain, to the best knowledge of the authors.

In the 2W-SSPE method, the propagation direction in the standard one-way SSPE is simply switched back-and-forth to model multipath effects over an irregular terrain [14, 15]. After the initial field is defined at a reference range, it is propagated in the forward direction until it hits the terrain, and then, it is decomposed into both forward and backward propagating waves. The forward field is set to zero on vertical positions where the terrain exists and is propagated in the forward direction in a similar manner. The backward field is initiated after imposing the boundary conditions on the terrain and making the field zero on vertical positions where the terrain does not exist. The backward field is marched out in the  $-x$  direction, and is computed by (2) where the signs of  $k$  and  $\Delta x$  are reversed. When the signs are reversed, we obtain the same equation except that the unknown field is expressed as  $\varphi_b(x, z) = u_b(x, z) \exp(-ikx)$  where the subscript- $b$  refers to the backward propagation. This process is repeated at each time the field hits the terrain. Finally, the total field is computed by superimposing all backward and forward propagating fields in the computation domain. This recursive algorithm is terminated when all backward and forward fields exit the domain or a certain threshold defined based on the difference between the total fields in consecutive steps is reached.

## 2.2. Method of moments

The MoM is an integral equation-based full-wave numerical method [23]. For horizontal (soft) polarization, i.e.  $\vec{E} = \hat{a}_y E_y(x, z)$  and  $H_y = 0$ , the electric field integral equation (EFIE) for perfectly conducting objects is expressed as follows:

$$\frac{k\eta}{4} \int_{C'} J_y(\vec{r}') H_0^{(1)}(k|\vec{r} - \vec{r}'|) d\ell' = E_y^i(\vec{r}), \quad (3)$$

where  $H_0^{(1)}$  is Hankel function of first kind and zeroth order,  $\vec{r}' = \hat{a}_x x' + \hat{a}_z z'$  and  $\vec{r} = \hat{a}_x x + \hat{a}_z z$  are the position vectors of the source and observation points, respectively,  $J_y$  is the induced current density on the surface,  $\eta$  is the intrinsic impedance,  $C'$  refers to the boundary of the object, and  $E_y^i(\vec{r})$  is the incident electric field.

By discretizing the boundary into  $N$  line segments where  $\Delta\ell \leq \lambda/10$  denotes the length of each line segment, and choosing the basis and weight functions as pulse and Dirac delta functions, respectively, a matrix equation  $[A][X] = [B]$  of size  $N \times N$  is constructed as follows:

$$A_{mn} = \begin{cases} \frac{k\eta}{4} H_0^{(1)}(kR_{mn}), & \text{for } m \neq n \\ \frac{k\eta}{4} \Delta\ell_m \left\{ 1 + i\frac{2}{\pi} \left[ \ln \left( \frac{\gamma k \Delta\ell_m}{4} \right) - 1 \right] \right\}, & \text{for } m = n \end{cases} \quad (4)$$

$$B_m = E_y^i(\vec{r}_m), \quad m, n = 1, 2, \dots, N$$

where  $\gamma = 1.7811$  is the Euler's constant,  $R_{mn} = \sqrt{(x_m - x_n)^2 + (z_m - z_n)^2}$  is the distance between the  $m$ -th and  $n$ -th segments, and  $\Delta\ell_m$  is the length of the  $m$ -th segment. The matrix equation is solved for the unknown

currents, i.e.  $X_n = J_y(\vec{r}_n)$ , and then, the currents are radiated to obtain the scattered fields.

For vertical (hard) polarization, i.e.  $\vec{H} = \hat{a}_y H_y(x, z)$  and  $E_y = 0$ , the magnetic field integral equation (MFIE) for perfectly conducting objects is given by

$$J_t(\vec{r}') - \frac{ik}{4} \int_{C'} J_t(\vec{r}') H_1^{(1)}(k|\vec{r} - \vec{r}'|) \left[ \sin \theta \frac{x - x'}{R} - \cos \theta \frac{z - z'}{R} \right] d\ell' = -H_y^i(\vec{r}), \quad (5)$$

where  $H_1^{(1)}$  is Hankel function of first kind and first order,  $J_t$  is the tangential component of the induced current density,  $\theta$  is the angle between the tangent vector  $\vec{t}(\vec{r}') = (\hat{a}_x \cos \theta + \hat{a}_z \sin \theta)|_{\vec{r}'}$  and the  $x$ -axis, and  $H_y^i(\vec{r})$  is the incident magnetic field. Similarly, a  $N \times N$  matrix equation is formed as follows:

$$A_{mn} = \begin{cases} \frac{ik\Delta\ell_n}{4} H_1^{(1)}(kR_{mn}) \left[ \sin \theta_n \frac{x_m - x_n}{R_{mn}} - \cos \theta_n \frac{z_m - z_n}{R_{mn}} \right], & \text{for } m \neq n \\ -\frac{1}{2}, & \text{for } m = n \end{cases} \quad (6)$$

$$B_m = H_y^i(\vec{r}_m), \quad m, n = 1, 2, \dots, N$$

which is then solved for the unknown currents  $X_n = J_t(\vec{r}_n)$ .

### 2.3. Hybrid method

The proposed hybrid method starts with the division of the computational domain into three regions, as shown in Figure 1b. The region-1 is between the transmitter antenna and the terrain/object. The region-2 is the region where the terrain/object is located. The region-3 is between the terrain/object and the end of the domain. In a typical propagation problem, the electrical size of the first and third regions are usually very large, which is not amenable to deal with standard full-wave numerical methods including MoM. Therefore, the SSPE method can effectively be used to propagate the fields over long distances in these regions. Since the second region includes curved surfaces, the MoM is used to better model such surfaces without staircasing approximation. The main steps of the hybrid algorithm are described below.

- In the first step, the incident field is obtained within the entire domain when there is no obstacle, by using the standard SSPE method discussed in subsection 2.1. In this manner, the incident fields,  $E_y^i(\vec{r})$  or  $H_y^i(\vec{r})$ , to be used as the excitation fields in MoM, are determined.
- In the second step, the MoM is employed by using the excitation fields obtained in the first step. In the MoM, the right-hand side of the matrix equation is constructed by using the fields determined in the first step. The matrix equation is solved for the induced current densities on the surface, which are then re-radiated to obtain the scattered fields at each range step (i.e. dashed lines in Figure 1c) in the second domain. Note that this is the range step used in the SSPE method, and hence it is electrically very large compared to the step size used in MoM. The blue and red curved arrows in Figure 1c are used to show the fact that the currents on the terrain surface are radiated to the left and right boundaries, respectively. The fields on the left and right boundaries are then propagated in the left and right directions, respectively.
- In the third step, the computed induced currents lying on the surface between two consecutive range steps are radiated by the MoM to obtain the fields at the corresponding range steps. For example, the currents

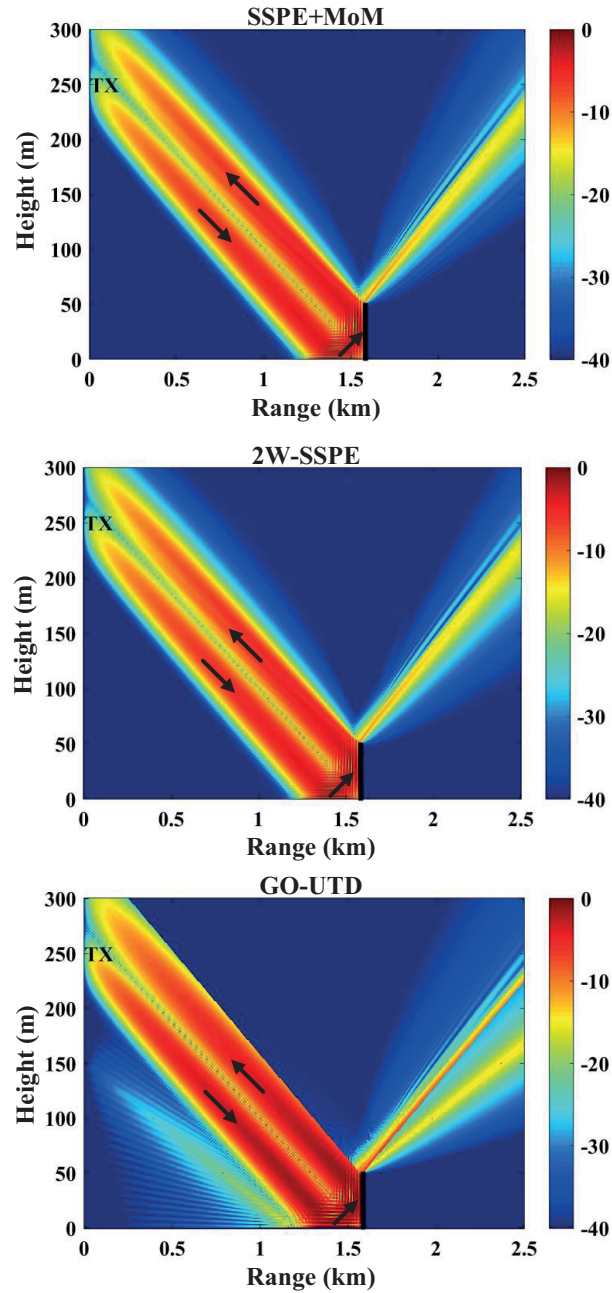


**Figure 2.** Propagation factor (PF) maps for example 1 with a knife-edge on the ground. The hybrid method (top), 2W-SSPE (middle), GO+UTD (bottom).

on the surface lying between the  $N$ -th and  $(N + 1)$ st range steps are used to determine the fields at these range steps. Next, the SSPE is employed to propagate the fields at the  $N$ -th and  $(N + 1)$ st range steps back and forth, respectively, in the absence of the terrain. This procedure is repeated for each range step and all field components are superimposed to obtain the field distribution in the entire domain.

It is useful to mention that the hybrid method can also be applied by modifying the third step as described



in [21]. That is, the currents on the entire terrain surface are radiated over the outermost boundaries of the second region, and the fields along these boundaries are marched back and forth in the first and third regions, respectively. When these two alternative hybridization schemes are compared, although the implementation of the approach given in [21] is simpler, it assumes that the atmosphere in the second region is homogeneous since the implementation of the MoM in inhomogeneous medium is not trivial due to the difficulty in defining the Green's function in such medium. However, in the proposed approach in this study, arbitrary refractivity profile can be defined in the second region since the SSPE is used to propagate the fields scattered from the terrain. Hence, inhomogeneous atmosphere and ducting effects can be modeled more accurately. The last example in Section 3 considers a propagation problem with ducting conditions.

### 3. Numerical examples

This section presents the results of some numerical experiments performed by the proposed method, the 2W-SSPE [14] and the GO+UTD [22] methods. In the examples, the frequency is 600 MHz, the antenna pattern is Gaussian with 3 dB beamwidth of  $0.5^\circ$  unless otherwise stated, the range step size is  $\Delta x = 5$  m, and the height step size is  $\Delta z = 0.2$  m. In MoM region, approximately one tenth of a wavelength is used as step size.

In the first example, a simple knife-edge is considered on the surface of a perfectly conducting ground surface. The transmitter antenna (TX) is placed at a height of 250 m and has the beam pointing angle of  $10^\circ$ . The propagation factor (PF) (i.e. the field strength relative to its free-space value), for horizontal polarization are shown in Figure 2. We expect that both 2W-SSPE and the hybrid methods work well because the obstacle does not have any curved/slanted geometry and is located on the ground surface. The reflections from the ground and the vertical lateral surface of the knife-edge are clearly observed and accurately modeled by both methods. The results are also similar to those of the GO+UTD method, with some differences along the reflection and shadow boundaries where the UTD method exhibits discontinuities due to the nature of the method.

In the second example, a triangular terrain is considered where the transmitter antenna is located at 200 m with the beam pointing angle of  $12^\circ$  and the 3 dB beamwidth of  $1^\circ$ . The PF maps for vertical polarization are shown in Figure 3. In the third example, a curved surface, which is modeled by a quarter sine function, is considered. The antenna is located at 200 m with the beam pointing angle of  $6^\circ$ . The PF maps for horizontal polarization are shown in Figure 4. It is clearly observed that the reflections from the tilted face of the triangular terrain in Figure 3 and the curved surface of the terrain in Figure 4 are modeled more accurately by the hybrid method compared to the 2W-SSPE method because the staircasing errors are removed. Especially, the result obtained by the 2W-SSPE in Figure 3b clearly shows that the reflection of the main beam from the terrain surface does not obey Snell's law of reflection due to the errors introduced by the staircasing approximation of the terrain geometry. The results of the hybrid method and the GO+UTD match well as expected.

From this point on, we demonstrate some representative examples where objects are located above the ground surface. As discussed before, the SSPE methods cannot easily model objects above the surface due to multiple images that need to be taken into account. In the fourth example, a rectangular object above the ground surface is demonstrated. The PF maps for horizontal polarization are shown in Figure 5. The antenna is located at 250 m with the beam pointing angle of  $10^\circ$ . It is obvious that the SSPE method is in difficulty in modeling reflections from the lower horizontal boundary of the object because the interactions between this surface and the ground are not properly modeled. However, the hybrid method can handle the strong field reflections in this region. Note that the GO+UTD results are not included because the GO+UTD toolbox is not designed for objects above the ground surface. However, since this and the following examples are designed



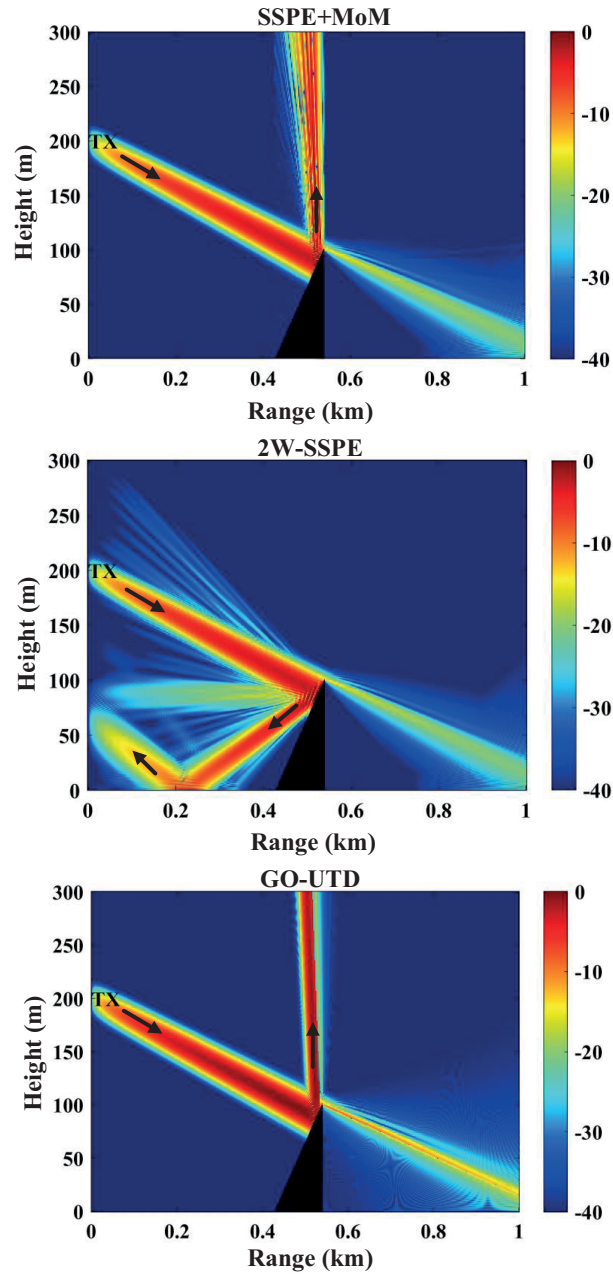


**Figure 3.** Propagation factor (PF) maps for example 2 with triangular terrain. The hybrid method (top), 2W-SSPE (middle), GO+UTD (bottom).

to produce strong reflections from flat surfaces, it is easy to verify the accuracy of the hybrid method by physical intuition.

The fifth example considers a horizontal boundary located at a height above the ground surface. The PF maps for horizontal polarization are shown in Figure 6. The antenna is located at 100 m with the beam pointing angle of  $15^\circ$  and the 3 dB beamwidth of  $1^\circ$ . Similar to the fourth example, the hybrid method can handle accurately the multipath effects between the object and the ground surface compared to the 2W-SSPE method

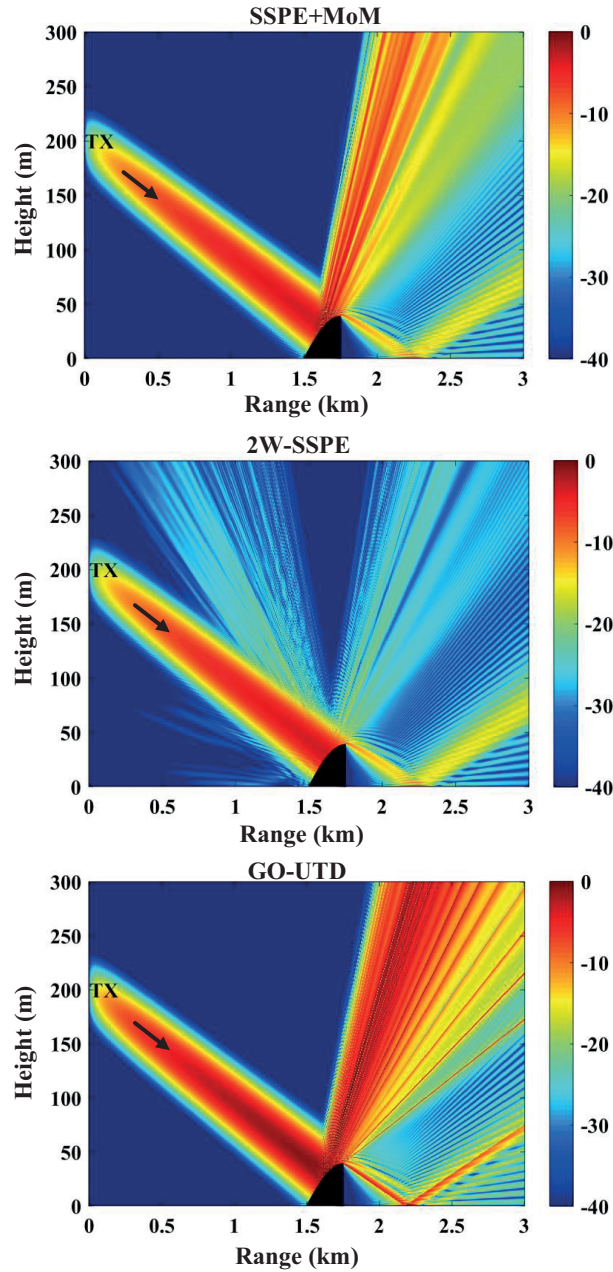


**Figure 4.** Propagation factor (PF) maps for example 3 with curved terrain modeled by a quarter sine function. The hybrid method (top), 2W-SSPE (middle), GO+UTD (bottom).

that cannot handle multiple images. In the last example, we assume that surface duct exists whose modified refractivity profile is shown in Figure 7. There exists a thin tilted object above the ground surface. The antenna is located at 50 m with the beam pointing angle of  $0^\circ$  and the 3 dB beamwidth of  $3^\circ$ . The polarization is horizontal. In the uppermost plot in Figure 7, the PF map corresponding to the standard SSPE over the entire domain is shown. Since there is not any object in this figure, the SSPE is run only in the forward direction. In fact, this result is used as an excitation field for MoM in the region where the object exists (i.e. in the region

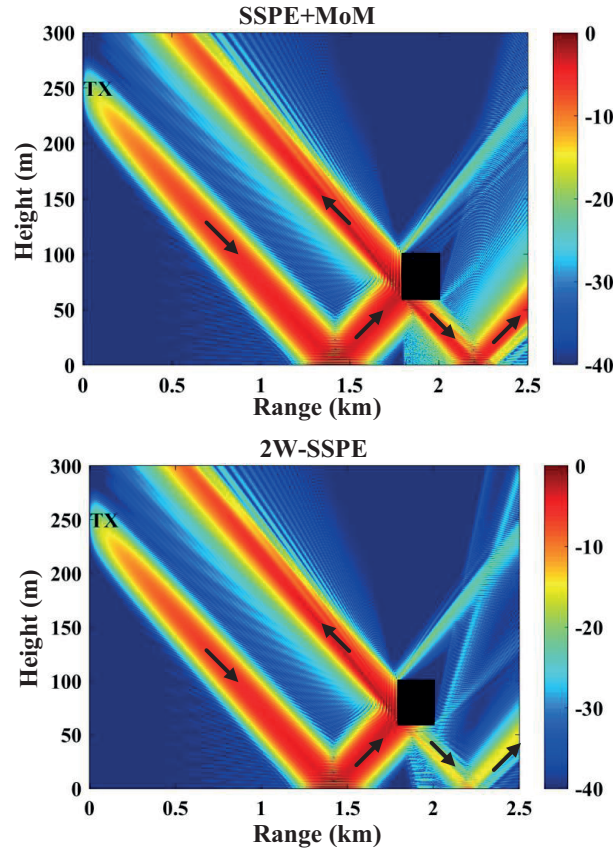


**Figure 5.** Propagation factor (PF) maps for example 4 with a rectangular object above ground. The hybrid method (top), 2W-SSPE (bottom).

between two dotted lines). The PF maps for the hybrid method and the 2W-SSPE method are also shown in this figure. Once again, we observe that the multipath effects between the tilted face of the object and the ground are modeled more accurately by the proposed hybrid method.

Finally, the computational load of the hybrid SSPE+MoM method is compared with the standard SSPE and MoM methods in Table 1. The simulations were performed on two Intel Xeon E5-2620 v3 CPUs with 64 GB of RAM. To measure the allocated memory, we have used the MATLAB profiler with undocumented options by typing the command `profile -memory on`. Furthermore, the hybrid and standard methods are qualitatively compared in Table 2 according to certain criteria. Although the standard SSPE is superior in terms of computational load (i.e. time and memory), its accuracy degrades when irregular terrain is modeled by staircase approximation and when there are objects above ground surface. Although the standard MoM provides very accurate results, it suffers from large computational load for long range propagation problems due to the need to use the step size criterion which is at most one-tenth of the wavelength. This is indeed a severe restriction when the range is on the order of several kilometers. For instance, the example in Figure 4 cannot be solved due to insufficient memory of the computer. Therefore, it is worthwhile to mention that the hybrid SSPE+MoM method has been originally proposed to combine the accuracy advantage of the standard MoM with the computational efficiency of the standard SSPE.

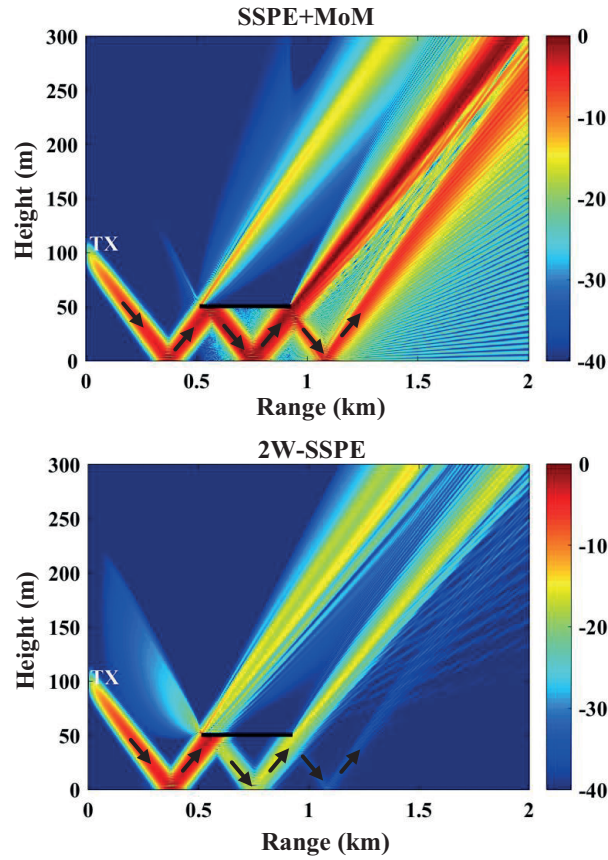


**Figure 6.** Propagation factor (PF) maps for example 5 with a horizontal boundary above ground. The hybrid method (top), 2W-SSPE (bottom).

**Table 1.** Computational load of the hybrid SSPE+MoM method compared to standard SSPE and MoM methods (In SSPE:  $\Delta x = 5\text{m}$  and  $\Delta z = 0.2\text{m}$ , in MoM:  $\Delta \ell \approx \lambda/10$ ).

Criterion	Method	Example 2 in Figure 3	Example 3 in Figure 4
Computation time	Hybrid SSPE+MoM	32 min	62 min
	Standard MoM	88 min	-
	Standard SSPE	40 sec	90 sec
Allocated memory	Hybrid SSPE+MoM	12 GB	42 GB
	Standard MoM	16 GB	out of memory
	Standard SSPE	7.5 GB	22 GB

#### 4. Conclusion

In this paper, a hybrid propagation model has been presented for modeling wave propagation in the troposphere. The hybrid method combines the advantages of the SSPE and MoM methods to increase the accuracy by eliminating the staircasing error in terrain modeling especially if the terrain includes curved/slanted boundaries. Furthermore, it allows us to solve problems involving objects above the ground surface, which cannot be modeled by the SSPE methods due to multiple images. The method has been applied to some representative propagation

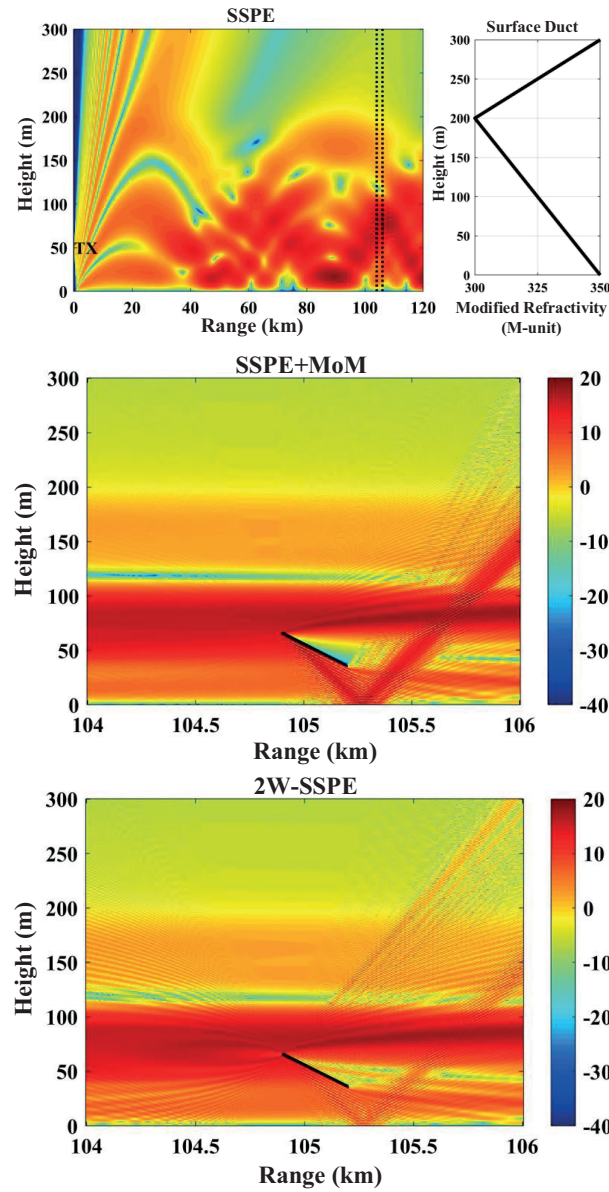


**Figure 7.** Propagation factor (PF) maps for example 6 with a tilted object above ground and in surface duct. The standard SSPE without object (top-left), modified refractivity of the surface duct (top-right), the hybrid method (middle), 2W-SSPE (bottom).

scenarios, and compared with the 2W-SSPE and GO+UTD methods. It has been observed that the scattered fields and multipath effects have been modeled accurately by the proposed hybrid method, in comparison to the 2W-SSPE method that employs staircasing approximation, when there are objects of irregular shape on/above the ground surface in standard atmosphere or even under ducting conditions. We have clearly shown that the staircasing approximation used in the standard SSPE may sometimes cause wave reflection to not obey Snell's law of reflection, and that the proposed hybrid method can improve the accuracy by better modeling curved surfaces. In addition, we have demonstrated that, when there are objects that do not touch the ground, the proposed method provides more accurate results than the standard SSPE, as it effortlessly overcomes



**Table 2.** Comparison of the hybrid SSPE+MoM method with standard methods by considering long range electromagnetic wave propagation problems involving objects on or above the ground surface.

Criterion	Hybrid SSPE+MoM	Standard MoM	Standard SSPE
Accuracy when irregular terrain exists	High	High	Medium
Modeling objects above ground surface	Yes	Yes	No
Modeling inhomogeneous atmosphere	Yes	No	Yes
Number of variables	Medium	High	Low
Memory requirement	Medium	High	Low
Computation time	Medium	Slow	Fast

the challenge of processing multiple images that should be included in the standard SSPE. In terms of the computational load (i.e. computation time and memory), the proposed method is between the standard SSPE and the standard MoM. It is more computationally efficient than the standard MoM because when the MoM is applied alone for the entire computational domain, very large number of unknowns must be introduced to satisfy the step size criterion of one-tenth of the wavelength for long range problems where the range extends to several kilometers. On the other hand, the standard SSPE is much faster than the proposed hybrid method and the standard MoM because electrically-large step size can be used throughout the range. Hence, the proposed method has been originally designed to overcome the trade-off between accuracy and computational load in standard SSPE and MoM methods. It is useful to note that the hybrid method can be accelerated further by using some special techniques to speed up the MoM implementation, such as fast multipole method or parallel processing methods. Here, we demonstrate the proof of concept that the hybrid method can be used to obtain more accurate and reliable results when irregular objects exist on/above the ground surface.

## References

- [1] Leontovich MA, Fock VA. Solution of propagation of electromagnetic waves along the Earth's surface by the method of parabolic equations. *Journal of Physics USSR* 1946; 10: 13-23.
- [2] Hardin RH, Tappert FD. Applications of the Split-Step Fourier method to the numerical solution of nonlinear and variable coefficient wave equations. *SIAM Review* 1973; 15: 423-423.
- [3] Feit MD, Fleck JA. Light propagation in graded-index optical fibers. *Applied Optics* 1978; 17 (24): 3990-3998. doi: 10.1364/AO.17.003990
- [4] Lee D, Pierce AD, Shang EC. Parabolic equation development in the twentieth century. *Journal of Computational Acoustics* 2000; 8: 527-637. doi: 10.1142/S0218396X00000388
- [5] Craig KH. Propagation modelling in the troposphere: parabolic equation method. *Electronics Letters* 1988; 24: 1136-1139. doi: 10.1049/el:19880773
- [6] Kuttler JR, Dockery GD. Theoretical description of the parabolic approximation/Fourier split-step method of representing electromagnetic propagation in the troposphere. *Radio Science* 1991; 26: 381-393. doi: 10.1029/91RS00109
- [7] Barrios E. A terrain parabolic equation model for propagation in the troposphere. *IEEE Transactions on Antennas and Propagation* 1994; 42: 90-98. doi: 10.1109/8.272306
- [8] Janaswamy R. A curvilinear coordinate-based split-step parabolic equation method for propagation predictions over terrain. *IEEE Transactions on Antennas and Propagation* 1998; 46: 1089-1097. doi: 10.1109/8.704813
- [9] Levy MF. *Parabolic Equation Methods for Electromagnetic Wave Propagation*. London: IEE Electromagnetic Wave Series 45, 2000.

- [10] Apaydin G, Sevgi L. The split step Fourier and finite element based parabolic equation propagation prediction tools: canonical tests, systematic comparisons, and calibration. *IEEE Antennas and Propagation Magazine* 2010; 52: 66-79. doi: 10.1109/MAP.2010.5586576
- [11] Zhang P, Bai L, Wu Z, Guo L. Applying the parabolic equation to tropospheric groundwave propagation: A review of recent achievements and significant milestones. *IEEE Antennas and Propagation Magazine* 2016; 58: 31-44. doi: 10.1109/MAP.2016.2541620
- [12] Thomson DJ, Chapman NR. A wide-angle split-step algorithm for the parabolic equation. *Journal of the Acoustical Society of America* 1983; 74: 1848-1854. doi: 10.1121/1.390272
- [13] Kuttler JR. Differences between the narrow-angle and wide-angle propagators in the split-step Fourier solution of the parabolic wave equation. *IEEE Transactions on Antennas and Propagation* 1999; 47: 1131-1140. doi: 10.1109/8.785743
- [14] Ozgun O. Recursive two-way parabolic equation approach for modeling terrain effects in tropospheric propagation. *IEEE Transactions on Antennas and Propagation* 2009; 47: 2706-2714. doi: 10.1109/TAP.2009.2027166
- [15] Ozgun O, Apaydin G, Kuzuoglu M, Sevgi L. PETOOL: MATLAB-based one-way and two-way split-step parabolic equation tool for radiowave propagation over variable terrain. *Computer Physics Communications* 2011; 182: 2638-2654. doi: 10.1016/j.cpc.2011.07.017
- [16] Ozgun O, Sahin V, Erguden ME, Apaydin G, Yilmaz AE et al. PETOOL v2.0: Parabolic Equation Toolbox with evaporation duct models and real environment data. *Computer Physics Communications* 2020; 256: 107454. doi: 10.1016/j.cpc.2020.107454
- [17] Dinc E, Akan OB. Beyond-line-of-sight communications with ducting layer. *IEEE Communications Magazine* 2014; 52: 37-43. doi: 10.1109/MCOM.2014.6917399
- [18] Lytaev MS. Nonlocal boundary conditions for split-step Pade approximations of the Helmholtz equation with modified refractive index. *IEEE Antennas and Wireless Propagation Letters* 2018; 17: 1561-1565. doi: 10.1109/LAWP.2018.2855086
- [19] Tepecik C, Navruz I. A novel hybrid model for inversion problem of atmospheric refractivity estimation. *International Journal of Electronics and Communications* 2018; 84: 258-264. doi: 10.1016/j.aeue.2017.12.009
- [20] Gilles MA, Earls C, Bindel D. A subspace pursuit method to infer refractivity in the marine atmospheric boundary layer. *IEEE Transactions on Geoscience and Remote Sensing* 2019; 57: 5606-5617. doi: 10.1109/TGRS.2019.2900582
- [21] Altun GY, Ozgun O. Electromagnetic propagation modeling over irregular terrain using a new hybrid method. In: *The 18th Mediterranean Microwave Symposium (MMS)*; İstanbul, Turkey; 2018. doi: 10.1109/MMS.2018.8612013
- [22] Ozgun O. New software tool (GO+UTD) for visualization of wave propagation. *IEEE Antennas and Propagation Magazine* 2016; 58: 91-103. doi: 10.1109/MAP.2016.2541600
- [23] Peterson AF, Ray SL, Mittra R. *Computational Methods for Electromagnetics*. New York: Wiley-IEEE Press, 1998.